

A SOLID-SOLUTION MODEL FOR Fe(II)-Fe(III)-Mg(II) GREEN RUSTS AND FOUGERITE AND ESTIMATION OF THEIR GIBBS FREE ENERGIES OF FORMATION

GUILHEM BOURRIÉ^{1,*}, FABIENNE TROLARD¹, PHILIPPE REFAIT² AND FRÉDÉRIC FEDER^{1,3}

¹ INRA, Unité de Recherche de Géochimie des Sols et des Eaux, URGSE, Europôle de l'Arbois, BP 80, F13545 Aix-en-Provence cedex 04, France

² LEMMA, Université de La Rochelle, Bâtiment Marie Curie, 25 rue Enrico Fermi, F17000 La Rochelle, France

³ CIRAD, Equipe “REGARD”, Station de La Bretagne, BP 20 F97408 Saint-Denis Messag, cedex 9, La Réunion, France

Abstract—Fe(II)-Fe(III) green rust identified in soil as a natural mineral is responsible for the blue-green color of gley horizons, and exerts the main control on Fe dynamics. A previous EXAFS study of the structure of the mineral confirmed that the mineral belongs to the group of green rusts (GR), but showed that there is a partial substitution of Fe(II) by Mg(II), which leads to the general formula of the mineral: $[Fe_{1-x}^{2+}Fe_x^{3+}Mg_y(OH)_{2+2y}]^{x+}[xOH^- \cdot mH_2O]^{x-}$. The regular binary solid-solution model proposed previously must be extended to ternary, with provision for incorporation of Mg in the mineral. Assuming ideal substitution between Mg(II) and Fe(II), the chemical potential of any Fe(II)-Fe(III)-Mg(II) hydroxy-hydroxide is obtained as: $\mu = X_1\mu_1^o + X_2\mu_2^o + X_3\mu_3^o + RT[X_1lnX_1 + X_2lnX_2 + X_3lnX_3] + A_{12}X_2(1 - X_2)$. All experimental data show that the mole ratio $X_2 = Fe(III)/[Fe_{total} + Mg]$ is constrained (1) structurally and (2) geochemically. Structurally, Fe(III) ions cannot neighbor each other, which leads to the inequality $X_2 \leq \frac{1}{3}$. Geochemically, Fe(III) cannot be too remote from each other for GR to form as $Fe(OH)_2$ and $Mg(OH)_2$ are very soluble, so $X_2 \geq \frac{1}{4}$. A linear relationship is obtained between the Gibbs free energy of formation of GR, normalized to one Fe atom, and the electronegativity χ of the interlayer anion, as: $\mu^o/n = -76.887\chi - 491.5206$ ($r^2 = 0.9985$, $N = 4$), from which the chemical potential of the mineral fougerite μ is obtained in the limiting case $X_3 = 0$, and knowing $\mu_1^o = -489.8 \text{ kJmol}^{-1}$ for $Fe(OH)_2$, and $\mu_3^o = -832.16 \text{ kJmol}^{-1}$ for $Mg(OH)_2$, the two unknown thermodynamic parameters of the solid-solution model are determined as:

$\mu_2^o = +119.18 \text{ kJmol}^{-1}$ for $Fe(OH)_3$ (virtual), and $A_{12} = -1456.28 \text{ kJmol}^{-1}$ (non-ideality parameter).

From Mössbauer *in situ* measurements and our model, the chemical composition of the GR mineral is constrained into a narrow range and the soil solutions-mineral equilibria computed. Soil solutions appear to be largely overstaured with respect to the two forms observed.

Key Words—Fe, Fougerite, Gley, Green Rust, Hydroxide, Mg, Model, Oxide, Soil, Thermodynamics.

INTRODUCTION

A green-blue color in soils has been used as a diagnostic criterion in the definition of gley and soil classification since the beginning of soil science, and ascribed immediately to the presence of Fe(II) oxide, called “protoxide”, by Vysotskii (1905, [1999]). The green-blue color of soils and sediments was ascribed to the presence of “the theoretical compound hydro-magnetite $Fe_3(OH)_8$ ” by Ponnampерuma *et al.* (1967) and more generally to double hydroxy-carbonate-GR by Taylor (1981). The discovery of these compounds in natural environments, specifically acid to neutral gley soils (Trolard *et al.*, 1996, 1997), has confirmed the hypothesis formulated by Vysotskii (1905) and demonstrated for the first time the existence of GR as a mineral. The mineral name “fougerite” has been approved by the Commission on New Minerals and Mineral Names of the International Mineralogical Association.

An extended X-ray absorption fine structure (EXAFS) study was recently undertaken on fougerite and synthetic GR and pyroaurites, which (1) confirmed that the mineral belongs to the GR group, but (2) led to the conclusion that it contains Mg(II) (which cannot be seen by Mössbauer spectroscopy) as well as Fe(II) and Fe(III) (Refait *et al.*, 2001). This was not taken into account in checking the soil-solution equilibria (Bourrié *et al.*, 1999) and in the solid-solution model proposed earlier (Génin *et al.*, 2001).

The aims of this paper are thus: (1) to derive a generalized ternary solid-solution model for Fe(II)-Fe(III)-Mg(II) GR and fougerite; (2) to discuss the structural and geochemical constraints that must satisfy this model; (3) to estimate the parameters of this model on the basis of experimental data available on GR and of a relation obtained between the Gibbs free energy of formation of GR and the electronegativity of the unhydrated interlayer anion; and (4) to apply the model to check soil solution-solid solution equilibria on the basis of field data.

* E-mail address of corresponding author:
bourrie@aix.inra.fr

DOI: 10.1346/CCMN.2004.0520313

STRUCTURE OF GREEN RUSTS AND STRUCTURAL CONSTRAINTS FOR A SOLID-SOLUTION MODEL

Structure of green rusts and of foougerite

Green rusts consist of brucite-like sheets of Fe(OH)_2 in which part of the Fe(II) is oxidized to Fe(III), the excess charge being compensated by interlayered anions; the interlayers are hydrated. Two types of structure – rhombohedral GR1 and trigonal GR2 – exist, depending on the nature of interlayered anions. With small spherical or planar anions such as chloride and carbonate, GR1 compounds are obtained, while with large tetrahedral anions, such as sulfate and selenate, GR2 compounds form (Génin *et al.*, 1998a; Simon *et al.*, 2003) (Figure 1).

The exact nature of the compensating anion in foougerite cannot be determined directly as its abundance is small (total Fe_2O_3 content in soil is only ~4%), the mineral is labile and cannot be separated from the other minerals and Mössbauer spectroscopy is only sensitive to Fe. From the composition of soil solutions analyzed in the localities where GR were identified, it was concluded that the most likely anion is simply OH^- . The structure was thus assumed to be analogous

to GR1(Cl), since OH^- is spherical as is Cl^- . Accordingly, the symmetry group was predicted to be the same as that of GR1(Cl), $R\bar{3}m$, with unit-cell parameters $a \approx 0.32$ nm and $c \approx 2.25$ nm, *i.e.* the same value for a , but a smaller value for c , due to the smaller size of OH^- (Génin *et al.*, 2001). In GR1(OH), the interlayer space can at most be completely filled with water molecules and OH^- ions that are of the same size, in a compact arrangement which leads to the complete general formula $[\text{Fe}_{1-x}^{2+}\text{Fe}_x^{3+}(\text{OH})_2]^{x+}[\text{xOH}^-\cdot m\text{H}_2\text{O}]^{x-}$, or globally Fe(OH)_{2+x} , with x ranging from $\frac{1}{3}$ to $\frac{2}{3}$, and $m \leq 1-x$. The Mössbauer and X-ray absorption spectroscopy (XAS) studies of foougerite have confirmed that it belongs to the GR1 group, but have shown that Mg substitutes for Fe in the mineral and that the local ratio of Mg/Fe is $\sim 2 \pm 1$. Its general structural formula must then be modified as: $[\text{Fe}_{1-x}^{2+}\text{Fe}_x^{3+}\text{Mg}_y(\text{OH})_{2+2y}]^{x+}[\text{xOH}^-\cdot m\text{H}_2\text{O}]^{x-}$, with $m \leq 1 - x + y$. As x is the parameter measurable by Mössbauer spectroscopy, the preceding notation will be used to discuss the corpus of available experimental data. However, the solid-solution model is more conveniently, and symmetrically, written on the basis of mole fractions of the three components Fe(OH)_2 , Fe(OH)_3 and Mg(OH)_2 respectively:

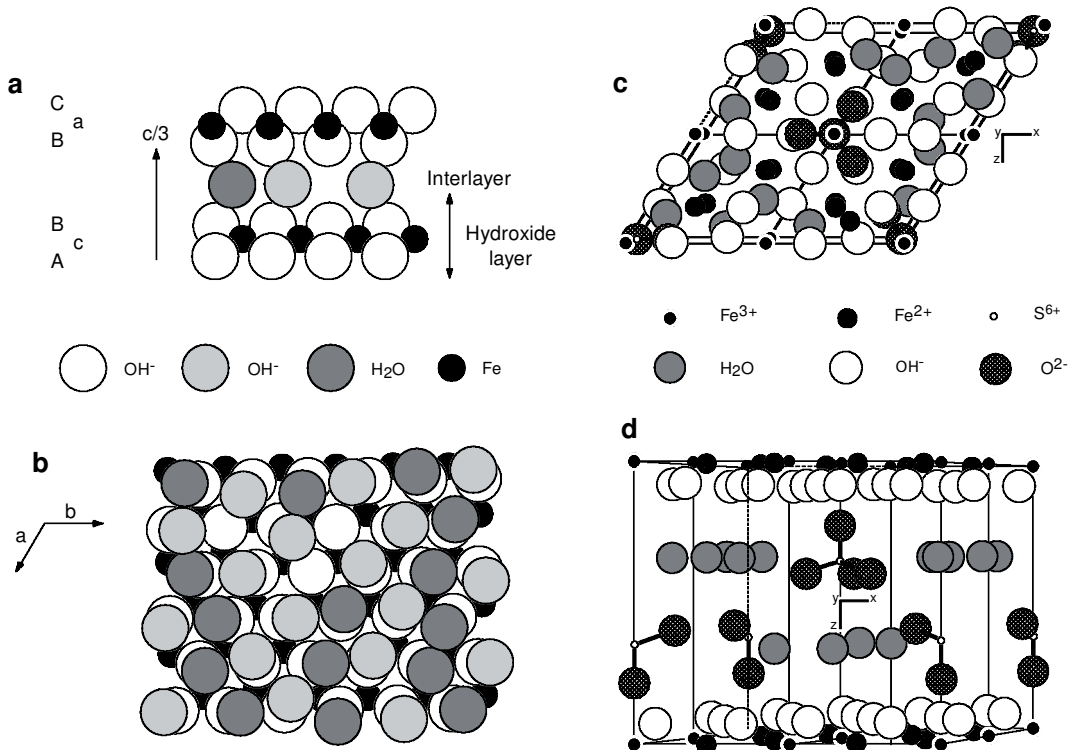


Figure 1. Structures of GR1 and GR2. (a) Stacking sequence for the crystal structure of the GR1(OH) mineral, foougerite, in the limiting case $\text{Fe}_3(\text{OH})_7$; (b) position of water molecules and OH^- ions in an interlayer viewed along [001]; only one interlayer, one OH^- and one Fe layer below are represented, from Génin *et al.* (2001); (c) projection of an ordered representation of the (2a, 2a, c) lattice of $\text{GR2}(\text{SO}_4^{2-})$ structure on the (001) plane; (d) stacking sequence for the crystal structure of $\text{GR2}(\text{SO}_4^{2-})$, from Simon *et al.* (2003).

$$X_1 = \frac{1-x}{1+y} \quad X_2 = \frac{x}{1+y} \quad X_3 = \frac{y}{1+y} \quad (1)$$

$$\frac{\text{Fe(II)} + \text{Mg(II)}}{\text{Fe(III)}} \geq 2 \iff \frac{1-y+y}{x} \geq 2 \iff x \leq \frac{1+y}{3} \quad (2)$$

The formula of fougereite can be written in a simplified way as: $(\text{Fe}^{2+}, \text{Mg})_{X_1+x_3}\text{Fe}^{3+}_{X_2}(\text{OH})_{2X_1+2X_2+3X_3}$

Structural constraints for the solid-solution model

From structural considerations, the smallest possible value for x is zero, which would correspond to a solid-solution between Fe(OH)_2 and Mg(OH)_2 . The effective ionic radii of Fe^{2+} and Mg^{2+} are very close to each other, 0.078 nm and 0.072 nm, respectively (Shannon, 1976), so that extensive substitution is possible. Indeed, most natural Fe(II) oxides, hydroxides and silicates admit continuous series between pure Fe(II) and Mg(II) end-members.

The upper limit for GR1(OH) was proposed as $x = \frac{1}{3}$ (Génin *et al.*, 2001). According to Vucelic *et al.* (1997), there exists a local ordering so that Fe^{3+} cations are never neighbors to each other. As each cation is surrounded by six cations, this means that this rule can be generalized now as: every Fe^{3+} must be surrounded by six bivalent cations, either Fe^{2+} or Mg^{2+} . The basic question is thus: what is the exact structural cause of this limitation?

For GR1(OH), the excess positive charge is compensated in the interlayer by deprotonation of the water molecule, the elementary reaction of oxidation being written in Figure 2. Further oxidation leading to two neighboring Fe(III) would then result in two neighboring OH^- in the interlayer (Figure 2). This is *a priori* structurally possible, but rather than deprotonating the remote interlayer water molecule, the repulsive field exerted by the two Fe(III) atoms would result in the deprotonation of the OH of the layer itself by an 'oxolation' process (Jolivet, 1994) and to $\text{Fe(III)}-\text{O}-\text{Fe(III)}$ bonds. The GR structure is then no longer stable and it transforms into magnetite with spinel inverse structure, or into an oxyhydroxide such as lepidocrocite (Olwe and Génin, 1991). Substitution of Fe(II) by Mg(II) in the structure stabilizes the green rust structure and the x mole ratio is allowed to increase to a limit given by the inequality:

which with equation 1 gives:

$$X_2 \leq \frac{1}{3} \quad (3)$$

The limiting case of pure Fe-GR. For $y = 0$, equation 2 simplifies to $x \leq \frac{1}{3}$, which corresponds to the global formula $\text{Fe}_3(\text{OH})_7$. This implies that the values obtained earlier for $x = \frac{1}{2}$ ' $\text{Fe}_2(\text{OH})_5$ ' and $x = \frac{2}{3}$ ' $\text{Fe}_3(\text{OH})_8$ ' must be ascribed in fact to $\text{Fe(II)}-\text{Fe(III)}-\text{Mg(II)}$ GR. It is worth noting that the GR synthesized heretofore without Mg have x values of $<\frac{1}{3}$ (Table 1), except in one case, GR1(Cl), with a slightly larger value ($x = 0.36$), which either is not significantly different from $x = \frac{1}{3}$ or would indicate that with some anions it is possible to accommodate a small increase of Fe(III). Moreover, in the case of selenate-GR2, the precipitate starts with $x = \frac{1}{3.25}$, then x increases to a maximum value $x = \frac{1}{3}$, over which it oxidizes into Fe(III) oxyhydroxides FeOOH .

It can thus be concluded that the inequality $x \leq \frac{1}{3}$ is satisfied when $y = 0$, from all the experimental results obtained so far. Any further oxidation leads to the formation of Fe oxyhydroxides, lepidocrocite, goethite, or akaganeite, or to the formation of magnetite-maghemit minerals. Similar conclusions apply also to compounds based on trivalent cations other than Fe. It is for example the case for synthetic meixnerite, $[\text{Mg}^{2+}_{1-x}\text{Al}^{3+}_x(\text{OH})_2]^{x+}[\text{x OH}^-(\text{OH})_2\text{H}_2\text{O}]^{x-}$, for which $0.23 \leq x \leq 0.33$ (Mascolo and Marino, 1980).

The general case of the ternary solid-solution. The Fe(III) mole fraction must be $<\frac{1}{3}$, which separates the excluded domain from the domain where it is structurally possible for GR to form. The inequality 2 can be drawn graphically in a triangular diagram in the system $\text{Fe}^{2+}(\text{OH})_2-\text{Fe}^{3+}(\text{OH})_3-\text{Mg}(\text{OH})_2$ (solid line, Figure 3).

For $y \geq 0$, i.e. when other divalent metals substitute for Fe(II), further oxidation is possible as soon as the inequality (3) is fulfilled. Such a compound was synthesized, with $x = \frac{1}{2}$ and $y = \frac{1}{2}$, by co-precipitation

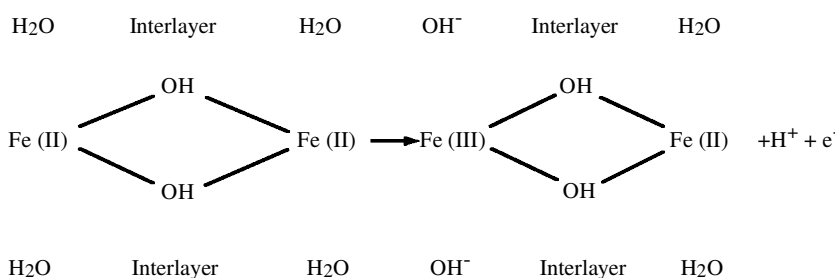


Figure 2. Modification of the composition of octahedra and interlayer in GR during the oxidation of Fe(II) to Fe(III).

Table 1. Structural formulae and Gibbs free energies of formation at 298.15 K and 1 bar of synthetic GR.

Structural formula	Group	x^*	$\mu^\circ \text{ exp.}$ (kJ mol ⁻¹)	$\mu^\circ \text{ calc.}^c$ (kJ mol ⁻¹)
[Fe ₃ ²⁺ Fe ³⁺ (OH) ₈] ⁺ [Cl ⁻ ·2H ₂ O] ⁻	GR1	1/4 ¹	-2145±7 ^a	-2132
[Fe ₂ ²⁺ Fe ³⁺ (OH) ₁₆] ²⁺ [SO ₄ ²⁻ ·4H ₂ O] ²⁻	GR1	1/4 ²	-	-5162
[Fe ₆ ²⁺ Fe ³⁺ (OH) ₁₆] ²⁺ [C ₂ O ₄ ²⁻ ·4H ₂ O] ²⁻	GR1	1/4 ³	-5383±3 ^b	-5365
[Fe ₅ ²⁺ Fe ³⁺ (OH) ₁₅] ²⁺ [SeO ₄ ²⁻ ·8H ₂ O] ²⁻	GR2	1/3,2 ⁴	-	-5007
[Fe ₂ ²⁺ Fe ³⁺ (OH) ₁₂] ²⁺ [SeO ₄ ²⁻ ·8H ₂ O] ²⁻	GR2	1/3 ⁴	-	-4006
[Fe ₄ ²⁺ Fe ³⁺ (OH) ₁₂] ²⁺ [SO ₄ ²⁻ ·8H ₂ O] ²⁻	GR2	1/3 ⁵	-3790±10	-3807
[Fe ₄ ²⁺ Fe ³⁺ (OH) ₁₂] ²⁺ [CO ₃ ²⁻ ·nH ₂ O] ²⁻	GR1	1/3 ^{6,7}	-3590±5 ^a	-3872

^a $x = \text{Fe(III)/Fe}_{\text{total}}$ mole ratio¹ Refait *et al.* (1998a); ² Simon *et al.* (1998); ³ Refait *et al.* (1998b); ⁴ Refait *et al.* (2000);⁵ Refait *et al.* (1999); ⁶ Hansen (1989); ⁷ Drissi *et al.* (1995)^a Bourrié *et al.* (1999); ^b ref. 3; ^c data from this paper

of Mg²⁺, Fe²⁺ and Fe³⁺ salts, at stoichiometry: [Fe₂²⁺Fe³⁺Mg²⁺(OH)₁₂]²⁺[CO₃²⁻·nH₂O]²⁻ (Refait *et al.*, 2001).

For $y = 1/2$, the limit is $x \leq 1/2$, which corresponds to the former formula 'Fe₂(OH)₅' and for $y = 1$, the limit is $x \leq 2/3$, which corresponds to the former formula 'Fe₃(OH)₈'. These compounds, whose Fe(III)/Fe_{total} ratios were observed in hydromorphic soils, can thus only be stable if they incorporate divalent cations other than Fe(II), for which Mg(II), due to its abundance in the environment is the more likely candidate. The proposed complete formulae for the mineral at remarkable points are given in Table 2 (points A, B, C, D, Figure 3), under the constraint that the total number of water molecules and OH⁻ ions is at most equal to the total number of

cations in the mole formula, with one monolayer of water in GR1-type compounds.

Larger Mg substitutions are possible, as this consists simply of diluting Fe atoms, and for $y \geq 2$, the complete oxidation of Fe is possible, which leads to a compound isomorphous with pyroaurite, with OH⁻ as a compensating anion instead of carbonate.

Among excluded forms are thus not only Fe(OH)₃, but all mixed Fe hydroxides Fe_{1-x}Fe³⁺(OH)_{2+x}, with $x \geq 1/3$, including the previously considered compounds Fe₂(OH)₅ and Fe₃(OH)₈ ("ferrosic hydroxide" of Arden, 1950). If they exist, the structure of these components instead of a GR structure, would be more consistent with the formula Fe(OH)₂·2FeOOH for "hydrated magnetite" used by Olowe and Génin (1991) and Refait and Génin (1993), which implies an oxolation of Fe(III)-Fe(III) bridges, but the structures of these hypothetical compounds are not established.

GEOCHEMICAL CONSTRAINTS

The solid-solution model proposed by Génin *et al.* (2001) must be revised given the presence of Mg in the mineral. This adds a degree of freedom to the system. The solid-solution is now ternary, and the end-members are the hypothetical minerals with a GR1 structure of the same composition as Fe(OH)₂ and Mg(OH)₂, but not

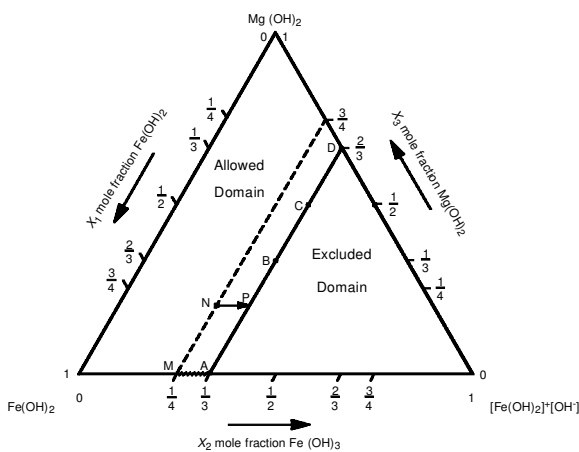


Figure 3. Diagram for the ternary system Mg(OH)₂-Fe(OH)₂-Fe(OH)₃. Solid line: limit between the excluded domain and the domain allowed for GR structure to be stable; dashed line: limit of the incipient precipitation of GR; M-A (hatched): interval of composition of synthetic GR. (A) Fe₃(OH)₇; (B) previously 'Fe₂(OH)₅' ≡ [MgFe²⁺Fe³⁺(OH)₆]⁺[OH⁻·mH₂O]⁻; (C) previously 'Fe₃(OH)₈' ≡ [Mg₃Fe²⁺Fe³⁺(OH)₁₂]²⁺[2OH⁻·mH₂O]²⁻; (D) limit with complete oxidation of Fe, [Mg₂Fe³⁺(OH)₆]⁺[OH⁻·mH₂O]⁻; (N-P) path of oxidation of fougérite (see text).

Table 2. Proposed structural formulae for the GR1(OH) mineral fougérite at remarkable points, and for the isomorphous OH analogue of pyroaurite.

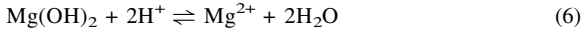
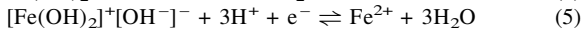
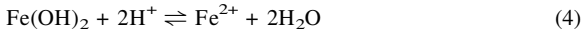
Structural formula (for $y = y_{\min.}$)	x	$y_{\min.}$	Ref. Fig. 3
[Fe ₂ ²⁺ Fe ³⁺ (OH) ₆] ⁺ [OH ⁻ ·mH ₂ O] ⁻	1/3	0	A
[Mg ₂ ²⁺ Fe ²⁺ Fe ³⁺ (OH) ₆] ⁺ [OH ⁻ ·mH ₂ O] ⁻	1/2	1/2	B
[Mg ₃ ²⁺ Fe ²⁺ Fe ³⁺ (OH) ₁₂] ²⁺ [2OH ⁻ ·mH ₂ O] ²⁻	2/3	1	C
[Mg ₂ ²⁺ Fe ³⁺ (OH) ₆] ⁺ [OH ⁻ ·mH ₂ O] ⁻	1	2	D

$x = \text{Fe(III)/Fe}_{\text{total}}$ mole ratio; $y = \text{Mg/Fe}_{\text{total}}$ mole ratio;
 $m \leq 1 - x + y$

necessarily with the same thermodynamic properties as their isomers of different structure.

Aqueous solution – ternary solid-solution equilibria

The equilibrium between a soil solution and a ternary solid-solution must be checked by writing a separate equilibrium equation for each pole:



In the following, indices 1, 2 and 3 will refer to Fe(II), Fe(III) and Mg(II) pure end-members, respectively. Ionic activity products (IAP) for each pole are defined by:

$$\log \text{IAP}_1 = \log (\text{Fe}^{2+}) + 2 \log a_w + 2 \text{pH} \quad (7)$$

$$\log \text{IAP}_2 = \log (\text{Fe}^{2+}) + 3 \log a_w + 3 \text{pH} + \text{pe} \quad (8)$$

$$\log \text{IAP}_3 = \log (\text{Mg}^{2+}) + 2 \log a_w + 2 \text{pH} \quad (9)$$

where quantities in parentheses are the activities of chemical species considered, a_w is the activity of water, pe is related to the redox potential measured with respect to the normal hydrogen electrode E_h , by $\text{pe} = (\text{FE}_h)/(\ln 10) \text{RT}$, T is the absolute temperature, $F = 96485.309 \text{ C mol}^{-1}$ and $R = 8.31451 \text{ Jmol}^{-1} \text{ K}^{-1}$.

At equilibrium, one has:

$$\log \text{IAP}_1 = \log K_1 + \log a_1 \quad (10)$$

$$\log \text{IAP}_2 = \log K_2 + \log a_2 \quad (11)$$

$$\log \text{IAP}_3 = \log K_3 + \log a_3 \quad (12)$$

where a_i is the activity of pole i in the solid-solution, which is different from unity, as the mineral is not a pure mineral in standard state. The activity coefficient λ_i of pole i in the solid-solution is defined by:

$$\lambda_i = a_i/X_i \quad (13)$$

where X_i is the mole fraction of pole i in the solid-solution, and the chemical potential of each pole in the solid solution is given by:

$$\mu_i = \mu_i^\circ + RT \ln X_i + RT \ln \lambda_i \quad (14)$$

The λ_i values are functions of P, T and the mole fractions of the solid X_i . The function defines the type of solid-solution.

For an ideal solid-solution, $\lambda_i = 1$. However, the end-members Fe(OH)_2 and Mg(OH)_2 have a brucite-like structure, with no intercalation of a monomolecular layer of water, but as soon as some Fe(II) is oxidized, the layers separate, hydrate and compensating anions enter the interlayer, which explains why the solid-solution is largely non-ideal (Génin *et al.*, 2001). As before, a regular solid-solution model will be used here.

Regular ternary solid-solution model for GR and fougérite

For a regular ternary solid-solution, the equations are (Prigogine and Defay, 1946, t. II p. 80):

$$RT \ln \lambda_1 = A_{12}X_2^2 + A_{13}X_3^2 + X_2X_3(A_{12}-A_{23}+A_{13}) \quad (15)$$

$$RT \ln \lambda_2 = A_{23}X_3^2 + A_{12}X_1^2 + X_1X_3(A_{12}+A_{23}-A_{13}) \quad (16)$$

$$RT \ln \lambda_3 = A_{13}X_1^2 + A_{23}X_2^2 + X_1X_2(-A_{12}+A_{23}+A_{13}) \quad (17)$$

where A_{ij} are the interaction parameters of the three binary solid-solutions. This implies that three parameters must be experimentally measured and fitted to a model of ternary regular solid-solution. For GR, we can make the assumption that the Fe(II)-Mg(II) substitution is ideal.

This implies that $\lambda_1 = \lambda_3$ for all X_2 and that if $X_2 = 0$, one obtains the ideal solid-solution Mg(II)-Fe(II), so that: $RT \ln \lambda_1 = A_{13}X_3^2 = 0$, hence $A_{13} = 0$. The same assumption implies that the effects of pole 1 and pole 3 on the activity coefficient of pole 2 are the same, i.e. $A_{12} = A_{23}$. One eventually obtains:

$$RT \ln \lambda_1 = A_{12}X_2^2 \quad (18)$$

$$RT \ln \lambda_2 = A_{12}(X_1 + X_3)^2 \quad (19)$$

$$RT \ln \lambda_3 = A_{12}X_2^2 \quad (20)$$

There remains only one adjustable parameter, $A_{12} = A_{23}$ and poles 1 and 3 play the same role, and this can be written equivalently as:

$$RT \ln \lambda_1 = A_{12}X_2^2 \quad (21)$$

$$RT \ln \lambda_2 = A_{12}(1 - X_2)^2 \quad (22)$$

$$RT \ln \lambda_3 = A_{12}X_2^2 \quad (23)$$

The chemical potentials of the three components and of the solid-solution are obtained as:

$$\mu_1 = \mu_1^\circ + RT \ln X_1 + A_{12}X_2^2 \quad (24)$$

$$\mu_2 = \mu_2^\circ + RT \ln X_2 + A_{12}(1 - X_2)^2 \quad (25)$$

$$\mu_3 = \mu_3^\circ + RT \ln X_3 + A_{12}X_2^2 \quad (26)$$

$$\mu = X_1 \mu_1 + X_2 \mu_2 + X_3 \mu_3 \quad (27)$$

The ideal and excess Gibbs free energy of mixing are given respectively by:

$$\Delta G_{\text{ideal}}/RT = X_1 \ln X_1 + X_2 \ln X_2 + X_3 \ln X_3 \quad (28)$$

$$\Delta G_{\text{excess}}/RT = X_1 \ln \lambda_1 + X_2 \ln \lambda_2 + X_3 \ln \lambda_3 \quad (29)$$

and by substituting equations 21–23 in equations 29 and 27, one obtains:

$$\Delta G_{\text{excess}} = A_{12} X_2 (1 - X_2) \quad (30)$$

$$\begin{aligned} \mu &= X_1 \mu_1^\circ + X_2 \mu_2^\circ + X_3 \mu_3^\circ \\ &\quad + RT [X_1 \ln X_1 + X_2 \ln X_2 + X_3 \ln X_3] \\ &\quad + A_{12} X_2 (1 - X_2) \end{aligned} \quad (31)$$

By letting $X_3 = 0$, one obtains the expression used to fit the regular solid-solution model previously (Génin *et al.*, 2001). The parameter A_{12} is identical to the parameter A_o obtained previously, though the value proposed previously must be revised as Mg was not considered in the computation of IAP values.

Difficulty in solving the system on the basis of aqueous solution-solid solution equilibria

In principle, the system can be solved by successive iterations for each aqueous solution to check equilibrium, if K_i are known, starting with $\lambda_i = 1$ and a tentative value of A_{12} .

The condition of equilibrium can thus be checked by computing first for each pole:

$$\log X_i = \log \text{IAP}_i - \log K_i - \log \lambda_i \quad (32)$$

and secondly by summing the X_i . The condition obtained is then:

$$\sum_i X_i < 1, \text{ the soil solution is undersaturated} \quad (33)$$

$$\sum_i X_i = 1, \text{ the soil solution is at equilibrium} \quad (34)$$

$$\sum_i X_i > 1, \text{ the soil solution is oversaturated} \quad (35)$$

This generalizes the classic condition $\text{IAP} < K$, $\text{IAP} = K$, $\text{IAP} > K$ for a pure solid (Bourrié, 1983).

The values of $\log \text{IAP}_i$ can be obtained from the composition of soil solution and the computation of activities and such a set of data is available (Bourrié et al., 1999). One must, however, know the values of K_i for pure end-members, which here it is not possible to measure directly as the purely ferric pole is virtual. Indeed, as the solubilities of Mg(OH)_2 and Fe(OH)_2 are very large, solutions are largely undersaturated with respect to these end-members, resulting in numerical instabilities. As explained before, the solid-solution is largely non-ideal, so that the values $\lambda_i = 1$ are not a good starting point for iterations. Moreover, the mineral is labile and cannot be separated, so that the mole fractions X_i are not measurable. Only the x mole ratio is measurable by Mössbauer spectroscopy.

Estimating both μ_2^\ominus , A_{12} and the X_i from a set of field data would imply the questionable assumption of equilibria at low temperature and give a circular character to the demonstration. Instead, hereafter, we will constrain the range of variation of the mole fraction X_2 better, then derive the chemical potential of the mineral, and eventually check equilibria independently with aqueous solutions.

Geochemical constraints on the solid-solution model

Lower limit of the mole fraction of Fe(III) in GR. On the basis of structural considerations, we have seen that the mole fraction of Fe(III) must be such that $X_2 \leqslant \frac{1}{3}$, as two Fe(III) must not be direct neighbors. Conversely, if X_2 is too small, the distance Fe(III)-Fe(III) is too large and the mineral will not form as the solubilities of Fe(OH)_2 and Mg(OH)_2 are very large. Experimentally, starting from Fe(OH)_2 , and letting it oxidize gently in contact with air, synthetic GR form in coexistence with Fe(OH)_2 from $x = \frac{1}{4}$.

With Ni(II), the compound obtained with the initial ratio $\text{Fe(II)}/\text{Ni(II)} = \frac{1}{3}$, i.e. $X_3 = \frac{3}{4}$, by assimilating Ni(II) to Mg(II) in Figure 3, is a GR1 isomorphous to GR1(Cl),

with $x = 1$, and $X_2 = \frac{1}{4}$ (Refaït and Génin, 1993). The unique product obtained corresponds to $X_2 = \frac{1}{4}$ (the point of intersection of the dashed line with the edge $\text{Mg(OH)}_2\text{-Fe(OH)}_3$ in the diagram). For larger initial ratios $\text{Fe(II)}/\text{Ni(II)}$, $\frac{1}{2}$ and 1, the initial products obtained bear $X_2 = \frac{1}{4}$ too.

In pyroaurite, $\text{Mg}_6^{2+}\text{Fe}_2^{3+}(\text{OH})_{16}\text{CO}_3\cdot 4\text{H}_2\text{O}$, $X_2 = \frac{1}{4}$; in GR1(CO_3), $\text{Fe}_x^{2+}\text{Fe}_2^{3+}(\text{OH})_{2x+4}\text{CO}_3\cdot n\text{H}_2\text{O}$, x ranges from four to six, ($X_2 = \frac{1}{4}$ to $\frac{1}{3}$) according to Murad and Taylor (1984), while $x = 4$ following Drissi et al. (1994) ($X_2 = \frac{1}{3}$). Similarly, when Al(III) substitutes for Fe(III), the product obtained by Taylor and MacKenzie (1980) is $\text{Fe}_6^{2+}[\text{Al}^{3+}, \text{Fe}^{3+}]_2(\text{OH})_{15.9}\text{Cl}_{1.85}$, with the mole ratio of trivalent ions $X_2 = \frac{1}{4}$, while in desautelite, synthesized by Hansen and Taylor (1991), $\text{Mg}_{8-x}\text{Mn}_x^{3+}(\text{OH})_{16}(\text{CO}_3^{2-})_{x/2}$, $2 < x < 2.67$, i.e. $\frac{1}{4} < X_2 < \frac{1}{3}$. As mentioned above, in synthetic meixnerite, Mg(II)-Al(III) compound, the mole ratio of trivalent ion obeys $0.23 \leqslant X_2 \leqslant 0.33$. It can thus be concluded that the formation of GR or more generally of pyroaurite-type compounds begins at the mole ratio: $X_2 \equiv M(\text{III})/[M(\text{III}) + M(\text{II})] = \frac{1}{4}$.

The value $X_2 = \frac{1}{4}$ corresponds structurally for GR1(OH), to the minimum distance Fe(III)-Fe(III), $d = a\sqrt{3}$, where a is the parameter of the hexagonal structure (Refaït et al., 2001). We will thus consider that the lower limit for the mole ratio X_2 is geochemically constrained to $\frac{1}{4}$, and that the upper limit is structurally constrained to $\frac{1}{3}$. The domain of composition of either synthetic or natural GR is thus limited by $X_2 = \frac{1}{4}$ (dashed line in Figure 3) and $X_2 = \frac{1}{3}$ (solid line in Figure 3).

Minimization of the chemical potential of GR and a relationship between A_{12} and the chemical potentials of pure end-members. We can now assume that the chemical potential of GR is minimal in the range $X_2 = [\frac{1}{4}, \frac{1}{3}]$, which is rather narrow. This is true even for a pure Fe(II)-Fe(III) system. When expressed as a function of mole fractions, one has:

$$\mu \equiv G/n = X_1 \mu_1 + X_2 \mu_2 \quad (36)$$

and by taking the derivative with respect to X_2 , one obtains (Prigogine and Defay, 1946, t. II, p. 12):

$$\frac{\partial \mu}{\partial X_2} = \mu_2 - \mu_1 \quad (37)$$

The derivative is zero for $X_2 = X_{2,\min.}$, which can be combined with equations 14, 21 and 22 and solved for A_{12} , and eventually gives:

$$A_{12} = \frac{[\mu_1^\ominus - \mu_2^\ominus - RT \ln(\frac{X_{2,\min}}{1-X_{2,\min}})]}{(1-2X_{2,\min})} \quad (38)$$

⇓

$$A_{12} = \frac{[\frac{\mu_1^\ominus - \mu_2^\ominus}{RT} - \ln(\frac{X_{2,\min}}{1-X_{2,\min}})]}{(1-2X_{2,\min})} \quad (39)$$

By taking as an average $X_{2,\min} = 7/24 \pm 1/24$, a linear relation is obtained between A_{12} and the Gibbs free energies of formation of the ferrous and ferric end-members. As a first approximation, $(\mu_1^\circ - \mu_2^\circ)/RT$ can be considered as constant, so that from equation 39, A_{12} can be computed at any temperature. There now remains one unknown parameter instead of two.

Constraints on the chemical potentials of pure end-members. The pure end-members are Fe(OH)_2 for which $\mu_1^\circ = -489.8 \text{ kJ mol}^{-1}$ at 298.15 K, 1 bar, from Bourrié *et al.* (1999) and $\text{Fe(OH)}_3 \equiv [\text{Fe}^{3+}(\text{OH})_2]^+[\text{OH}^-]^-$. However, as this end-member is virtual, μ_2° is not measurable. This value must, however, be more positive than the values for lepidocrocite and goethite with one water molecule added, and hematite, with two water molecules added, which are the stable or metastable phases. Taking $-470.7 \text{ kJ mol}^{-1}$ for lepidocrocite (Hashimoto and Misawa, 1973), $-480.3 \text{ kJ mol}^{-1}$ for goethite (Dé tourneau *et al.*, 1975), $-755.45 \text{ kJ mol}^{-1}$ for hematite (Bratsch, 1989) and $-237.18 \text{ kJ mol}^{-1}$ for liquid water (Wagman *et al.*, 1982), one obtains a minimum value $\mu_2^\circ > -708 \text{ kJ mol}^{-1}$. The value previously proposed was $\mu_2^\circ = -641 \text{ kJ mol}^{-1}$ (Génin *et al.*, 2001), but Mg was not considered in the mineral. Instead, for GR to form, A_{12} must be negative, which implies $\mu_2^\circ > -490 \text{ kJ mol}^{-1}$, by letting $X_2 = X_{2,\min} = 7/24$ in equation 39. The value of μ_2° is thus not constrained enough to give a reliable value of A_{12} from equation 31. The previously published value $\mu_2^\circ = -641 \text{ kJ mol}^{-1}$ (Génin *et al.*, 2001) leads to $X_{2,\min} = 7/3$, which is inconsistent with the structural constraints, and must be discarded.

The only way to solve the system is then to obtain a value for μ for the mineral in the range of variation of X_2 where GR exist, but as the natural mineral fouggerite is labile and cannot be separated, and to date has not been synthesized, this value must be estimated from the values measured on synthetic GR.

ESTIMATION OF THE GIBBS FREE ENERGY OF FORMATION OF GR1-OH

General relation between the Gibbs free energies of formation of synthetic GR and the electronegativities of anions taken on the Allred-Rochow scale

The experimental values of the Gibbs free energies of formation of synthetic GR are reported in Table 1 at 298.15 K, 1 bar. As these compounds are essentially isostructural, we can look for a relationship between this thermodynamic property and a suitable parameter. The changes are essentially the nature of the interlayered anion, the number of moles of water, which depends on the type of GR, and to a lesser degree the mole ratio X_2 . Those factors are closely correlated, and the nature of the anion is the main factor. As the interactions between the layer and the anion are of electrostatic nature, we chose the electronegativity of the anion as a parameter.

More specifically, we used the Allred and Rochow electronegativity scale, as it is based on the energetics of interaction between a molecule or an ion and the electron and is a function of the global charge Z of the molecule or ion. We follow the model of partial charges developed by Jolivet (1994). Given the electronegativities χ_i^* of the elements, the electronegativity of a molecule is obtained as:

$$\chi = \frac{\sum_i \sqrt{\chi_i^*} + 1.36Z}{\sum_i \frac{1}{\sqrt{\chi_i^*}}} \quad (40)$$

With $\chi_i^* = 2.50$ for C and Se, 3.50 for O, 2.83 for Cl, 2.48 for S (Jolivet, 1994) the values obtained for the anions are $\chi = 0.54$ for Cl^- , 1.86 for SO_4^{2-} , 2.0 for CO_3^{2-} and SO_3^{2-} , 2.29 for SeO_4^{2-} and 2.33 for oxalate $\text{C}_2\text{O}_4^{2-}$. The Gibbs free energies of formation of synthetic GR, normalized to 1 Fe atom, are plotted vs. the Allred-Rochow electronegativities of the interlayer anions in Figure 4. The value of the Gibbs free energy of formation of Fe(OH)_2 is plotted at $\chi = 0$, as the interlayer is empty.

All points except $\text{GR1}(\text{CO}_3)$ and including Fe(OH)_2 and $\text{GR2}(\text{SO}_4)$ are perfectly aligned, along a straight line following the empirical law:

$$\frac{\mu^\circ}{n} = -76.887\chi - 491.5206, r^2 = 0.9985, N = 4 \quad (41)$$

where n is the number of Fe atoms per mole formula, and μ° is in kJ mol^{-1} . The differences between calculated

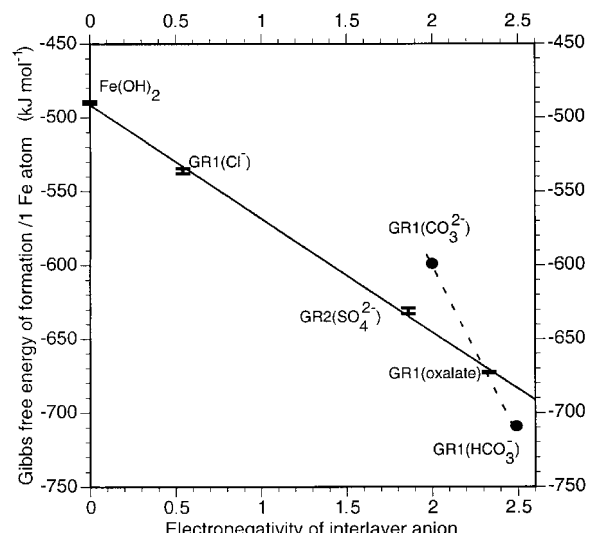


Figure 4. Relation between Gibbs free energy of formation of synthetic GR (see Table 1), normalized to one Fe atom/mole formula and the Allred and Rochow electronegativity of the interlayer anion, computed following the model of partial charges (Jolivet, 1994) (see text, equation 40). Solid line: linear regression through all points (error bars) except $\text{GR1}(\text{CO}_3)$ (see equation 41); black circles: Gibbs free energy of formation of $\text{GR1}(\text{CO}_3)$ (Table 1) at $\chi = 2$ and recalculated from experimental data (Table 3) as $\text{GR1}(\text{HCO}_3)$ (reaction 42), at $\chi = 2.49$; the dashed line connects those two extreme values for carbonate GR.

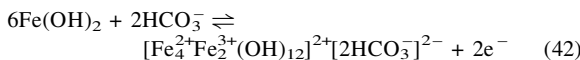
and experimental values are within 0.6% (Table 1) except for GR1(CO_3^-), which will be discussed just below. It is remarkable that: (1) the value for $\text{Fe}(\text{OH})_2$ plotted at $\chi = 0$ is aligned with GR; (2) that GR2(SO_4^{2-}) is aligned with GR1s.

This confirms that the main factor is the nature of the anion. The stacking differences between the two types of GR and the number of molecules of water are not reflected in the dispersion. Considering the number of molecules of water and computing the electronegativities of $\text{Cl}^- \cdot 2\text{H}_2\text{O}$, etc. resulted in a large scattering of points in the diagram. The normalized Gibbs free energies of formation of GR are thus entirely explained by the electronegativity of the non-hydrated anion.

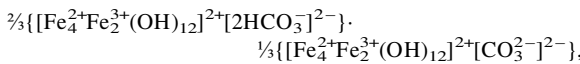
Gibbs free energy of formation of GR1(CO_3^-)

For GR1(CO_3^-), the discrepancy is 8% and is largely out of range of the experimental uncertainty, i.e. $\pm 11 \text{ kJ mol}^{-1}$. The experimental value is derived from measurements of E_h and pH at equilibrium between $\text{Fe}(\text{OH})_2$ and the synthetic GR from Drissi *et al.* (1994) (Table 3).

The equilibrium was considered between GR1(CO_3^-) and $\text{Fe}(\text{OH})_2$. If however, HCO_3^- was the interlayer anion, the formula of the GR would be $[\text{Fe}_4^{2+}\text{Fe}_2^{3+}(\text{OH})_{12}]^{2+}[2\text{HCO}_3^-]^{2-}$, and the equilibrium with $\text{Fe}(\text{OH})_2$ would be:



from which the data from Table 3 can be used to give $\mu^\circ = -4248.23 \pm 3 \text{ kJ mol}^{-1}$. This value, when normalized to one Fe atom and plotted at $\chi(\text{HCO}_3^-) = 2.49$ is below the general regression line. Carbonate GR could thus indeed be a mixed CO_3^{2-} - HCO_3^- GR. The intersection between the solid line and dashed line in Figure 4 leads to an average value $\chi = 2.32 = \frac{1}{3}\chi(\text{HCO}_3^-) + \frac{1}{3}\chi(\text{CO}_3^{2-})$. The formula for GR1(CO_3^-) could thus be:



or equivalently:

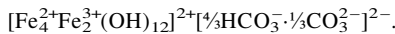


Table 3. Experimental data used to reevaluate the Gibbs free energy of formation of GR1(CO_3^-), from Drissi *et al.* (1994).

$R = \text{OH/Fe}$	$E_h (\text{V})^a$	pH^a	$a(\text{CO}_3^{2-})^a$	$\log a(\text{HCO}_3^-)^b$	$\log K^c$	$\Delta_R G^\circ d$	$\mu^\circ e$
0.545	-0.598	10.82	0.027	-2.059	24.34	-138.896	-4251.24
0.600	-0.597	10.20	0.015	-1.694	23.57	-134.539	-4246.88
0.615	-0.596	10.19	0.015	-1.684	23.52	-134.232	-4246.57
Average	-0.597	10.40	0.019	-1.812	23.807	-135.89	-4248.23
σ	0.001	0.36	0.007	0.214	0.457	2.61	2.61

^a Drissi *et al.* (1994)

^b computed as $\log a(\text{HCO}_3^-) = \log a(\text{CO}_3^{2-}) - \text{pH} + 10.33$

^c $\log K = -2[F\text{E}_h/(\ln 10)\text{RT} - 2\log a(\text{HCO}_3^-)]$

^d $\Delta_R G^\circ = -(\ln 10)\text{RT} \log K$

^e computed from $\mu^\circ = \Delta_R G^\circ + 2\mu^\circ(\text{HCO}_3^-) + 6\mu^\circ(\text{Fe}(\text{OH})_2)$, with $\mu^\circ(\text{HCO}_3^-) = -586.77 \text{ kJ mol}^{-1}$ from Wagman *et al.* (1982) and $\mu^\circ(\text{Fe}(\text{OH})_2) = -489.8 \text{ kJ mol}^{-1}$ from Bourrié *et al.* (1999).

The activity ratio $[\text{HCO}_3^-]/[\text{CO}_3^{2-}] = 4$ in the interlayer, corresponds to $\text{pH} = 9.73$, which is 0.5 to 1.1 lower than the pH in the external solution, which can be ascribed to the classical surface acidity of the positively charged interlayer. There is no steric hindrance, as there are six Fe atoms, so there is space for six H_2O molecules, i.e. six O. In the formula proposed, there are five O, so there is the possibility of having at most one water molecule in addition in the cell. From the value $\chi = 2.32$, and equation 41, we obtain $\mu^\circ = -4018 \text{ kJ mol}^{-1}$ for GR1($\frac{1}{3}\text{HCO}_3^- \cdot \frac{2}{3}\text{CO}_3^{2-}$) at 298.15 K, 1 bar. However, the mole ratio $\text{Fe(III)}/\text{C}$ would then be $2/(\frac{1}{3}) = 1.2$ instead of 2 as generally admitted. Thus, either the stoichiometry or the chemical potential of the hydroxy-carbonate GR must be reevaluated.

It must be noted that the intersection of the carbonate data with the regression line in Figure 4 occurs at the same point where the oxalate data point occurs. As the oxalate and carbonate functional groups are rather similar, this strengthens the main importance of the nature of the interlayer anion.

From equation 41, with $\chi(\text{SO}_4^{2-}) = 2$ and $\chi(\text{SeO}_4^{2-}) = 2.29$, we obtain the Gibbs free energies of formation of the other synthetic GR: GR1(SO_4^{2-}), GR2(SeO_4^{2-}) which are reported in Table 1, for which no published data are available.

Estimation of the Gibbs free energy of formation of the purely ferroso-ferric GR1(OH)

From equation 41, with $\chi(\text{OH}^-) = 1.60$, we eventually obtain $\mu = -614.5 \text{ kJ mol}^{-1}$ for GR1(OH), with one Fe atom per mole formula. This value, near the minimum at the limit $X_3 = 0$ (no Mg in fougérite) is in the range of values proposed previously for $\text{Fe}_3(\text{OH})_7$, i.e. $-1799.7 \text{ kJ mol}^{-1}$ or $-600 \text{ kJ mol}^{-1}/1 \text{ Fe atom}$, and for ' $\text{Fe}_2(\text{OH})_5$ ', i.e. $-1244.1 \text{ kJ mol}^{-1}$ or $-622 \text{ kJ mol}^{-1}/1 \text{ Fe atom}$, but it must be preferred, as it is based on carefully controlled experiments on synthetic GR, thermodynamics of solid-solutions and the model of partial charges.

THE COMPLETE TERNARY SOLID-SOLUTION MODEL FOR Fe(II)-Fe(III)-Mg(II) GR

From the value of μ , we can solve entirely the binary regular solid-solution model. From equation 37, we have at the minimum, $\mu_1 = \mu_2$ and from equation 36, with $X_1 + X_2 = 1$, we obtain:

$$\mu = \mu_1 = \mu_2 = -614.5 \text{ kJ mol}^{-1} \quad (43)$$

whose physical meaning is that μ is minimal when the chemical potentials of the components of the binary solid-solution are identical.

With $X_1 = 17/24$, $X_2 = 7/24$ and $\mu_1^\circ = -489.8 \text{ kJ mol}^{-1}$, by inserting the value of μ_1 in equation 24, we obtain $A_{12} = -1456.28 \text{ kJ mol}^{-1}$, and by inserting the value of μ_2 in equation 25, we obtain $\mu_2^\circ = +119.18 \text{ kJ mol}^{-1}$.

As expected, A_{12} is negative, which implies that GR will not demix at any temperature (Prigogine and Defay, 1946). The positive value for μ_2° implies that a GR structure for Fe(OH)_3 is absolutely impossible. Electrostatic repulsions would be so large that this compound would be unstable with respect to the elements in their standard state, metallic Fe, $\text{O}_{2,\text{gas}}$ and $\text{H}_{2,\text{gas}}$! Indeed, this simply means that an octahedral packing of OH cannot accommodate neighboring Fe(III) and that deprotonation of OH leads by an oxidation process to other iron oxides.

The A_{12} value obtained is larger than the corresponding value for $\text{FeO}-\text{MgO}$, i.e. $+15.945 \text{ kJ mol}^{-1}$ (Davies and Navrotsky, 1983), and of opposite sign. However, this latter value is relative to the halite-like structure of oxides and valid at high temperatures (1373–1573 K). Moreover, it refers to a substitution of same-charge cations, Fe(II)-Mg(II). Our value, largely negative, refers to the simultaneous substitution $\text{Fe(II)}\cdot\text{H}_2\text{O}\cdot\text{Fe(III)}\cdot\text{OH}$ (see Figure 1) and implies much more important changes in the electronic structure of the solid, so that the values cannot be directly compared. The large negative value of A_{12} we obtained compensates the positive value of μ_2° and makes the fougere stable.

Our solid-solution model for GR is now complete with the value for the pure Mg(OH)_2 end-member, for

which we take the value of brucite, $\mu_3^\circ = -832.16 \text{ kJ mol}^{-1}$, from Altmeier *et al.* (2003). The basic equation of the model and the parameters are summarized in Table 4.

CHECK OF SOIL SOLUTION-FOUGERITE EQUILIBRIUM

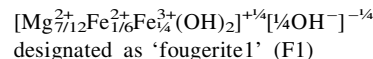
Soil solution was studied in the site where fougere was discovered (Trolard *et al.*, 1996, 1997), in a gley soil developed on granite at Fougères (Brittany, France) and simultaneously three types of data were measured (Feder, 2001): (1) Mössbauer spectra were acquired in the field at different depths and times; (2) E_h and pH were monitored in the groundwater at 70 cm depth every hour, in a gley horizon; (3) the soil solution was sampled every week or twice a month for complete analysis.

Mössbauer spectra show clear evidence of the presence of fougere, and the mole ratio $x = \text{Fe(III)}/\text{Fe}_{\text{total}}$ in the mineral decreases monotonically with depth, from 0.64 to 0.34, as the milieu becomes more and more reducing. At a given depth, when repeated measurements are made at different times, significant variations of x are observed, though the amplitude is smaller than the entire variation in the profile. No values were observed outside the range $x = [\frac{1}{3}, \frac{2}{3}]$.

At the depth where the composition of soil solution was monitored, x ranges from 0.59 to 0.61.

By definition, $x = X_2/(X_1 + X_2)$; hence with $x = 0.6$, $X_1 = 2X_2/3$. According to our model, $\frac{1}{4} \leq X_2 \leq \frac{1}{3}$. With $X_2 = \frac{1}{4}$, we obtain: $X_1 = \frac{1}{6}$, and $X_3 = \frac{1}{12}$. With $X_2 = \frac{1}{3}$, we obtain: $X_1 = \frac{1}{3}$, and $X_3 = \frac{1}{3}$.

By combining the data from Mössbauer spectroscopy in the field and the structural and geochemical constraints for fougere composition, we can thus solve the system and obtain the three mole fractions of the components. The range of composition of fougere at that depth is thus between:



and

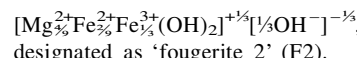


Table 4. Basic equation and parameters of the regular ternary solid-solution model for hydroxy- $\text{Fe(II)}\cdot\text{Fe(III)}\cdot\text{Mg(II)}$ GR, fougere, at 298.15 K and 1 bar.

Equation
$\mu = X_1\mu_1^\circ + X_2\mu_2^\circ + X_3\mu_3^\circ + RT [X_1 \ln X_1 + X_2 \ln X_2 + X_3 \ln X_3] + A_{12}X_2 (1 - X_2)$, (equation 31)
Thermodynamic parameters
Fe(OH) ₂
Fe(OH) ₃ (virtual)
Mg(OH) ₂
Non-ideality parameter

$$\begin{aligned} \mu^\circ &= -489.8 \text{ kJ mol}^{-1} \\ \mu^\circ &= +119.18 \text{ kJ mol}^{-1} \\ \mu^\circ &= -832.16 \text{ kJ mol}^{-1} \\ A_{12} &= -1456.28 \text{ kJ mol}^{-1} \end{aligned}$$

Table 5. Geochemical characteristics of soil solutions from Fougères (Feder, 2001) ($N = 68$).

Date	T (K)	pH	pe	$\log (\text{Fe}^{2+})$	$\log (\text{Mg}^{2+})$	$\log \text{IAP}_{\text{FI}}$	$\log \text{IAP}_{\text{F2}}$
February 19 1999	280.15	7.3	-3.171	-3.2192	-3.682	29.14	22.59
February 22 1999	280.75	7.24	-3.162	-3.2669	-3.7055	28.74	22.28
February 26 1999	280.75	7.12	-3.298	-3.1798	-3.7981	27.97	21.71
March 1 1999	280.75	7.11	-3.297	-3.3108	-3.8118	27.77	21.52
March 5 1999	281.15	7.15	-3.049	-3.495	-3.8474	27.9	21.63
March 8 1999	280.65	7.52	-2.975	-3.405	-3.9167	29.93	23.26
March 11 1999	280.75	7.16	-3.162	-3.4033	-3.8488	27.98	21.69
March 16 1999	281.45	7.19	-3.037	-3.3255	-3.8661	28.27	21.96
March 19 1999	281.55	7.15	-3.054	-3.3688	-3.8448	28.03	21.75
March 26 1999	281.65	7.12	-3.14	-3.3212	-3.8141	27.9	21.65
March 29 1999	281.85	7.1	-3.193	-3.3636	-3.8877	27.62	21.43
March 31 1999	281.85	7.08	-3.227	-3.574	-3.9257	27.23	21.09
April 6 1999	282.75	7.11	-3.205	-3.421	-3.875	27.63	21.42
April 14 1999	282.65	7.1	-3.069	-3.3455	-3.8794	27.72	21.53
April 22 1999	282.25	7.07	-2.911	-3.3949	-3.8852	27.6	21.44
April 26 1999	282.45	7.11	-2.948	-3.5895	-3.9202	27.55	21.37
April 30 1999	283.05	7.31	-3.311	-3.4456	-3.9432	28.52	22.12
May 6 1999	284.05	7.24	-3.339	-3.4326	-4.2152	27.76	21.6
May 12 1999	284.35	7.08	-3.225	-3.5259	-3.9408	27.25	21.12
May 19 1999	284.15	7.24	-3.206	-3.4911	-3.9631	28.13	21.82
May 26 1999	284.45	7.37	-3.108	-3.5162	-3.9127	28.94	22.44
June 2 1999	285.55	7.37	-3.072	-3.5067	-3.9095	28.97	22.48
June 9 1999	285.35	7.4	-3.103	-3.4819	-4.0459	28.95	22.5
June 14 1999	285.25	7.41	-3.152	-3.504	-4.1734	28.78	22.39
June 18 1999	285.65	7.36	-3.124	-3.529	-3.8986	28.88	22.39
June 21 1999	285.85	7.28	-3.076	-3.5506	-3.9309	28.41	22.04
June 28 1999	286.05	7.31	-3.112	-3.57	-3.9202	28.55	22.13
July 1 1999	286.15	7.24	-3.147	-3.4891	-3.9258	28.22	21.89
July 5 1999	286.65	7.19	-3.153	-3.5945	-3.9605	27.8	21.54
July 8 1999	286.75	7.18	-3.188	-3.576	-3.9579	27.74	21.5
July 13 1999	287.25	7.19	-3.262	-3.6222	-3.9249	27.75	21.48
July 19 1999	287.35	6.85	-3.28	-3.6148	-3.9439	25.89	20.03
July 27 1999	287.75	6.49	-3.489	-3.5465	-3.9449	23.88	18.46
August 16 1999	287.75	6.42	-3.489	-3.7836	-4.0035	23.19	17.88
August 20 1999	287.45	6.4	-3.468	-3.5966	-4.0463	23.22	17.97
August 23 1999	287.65	6.42	-3.471	-3.6374	-4.0463	23.28	18.01
August 27 1999	288.05	6.45	-3.475	-3.7095	-4.0562	23.36	18.05
September 20 1999	287.35	6.28	-0.508	-4.759	-4.2918	22.84	17.88
September 21 1999	287.35	6.3	-0.255	-4.6622	-4.292	23.2	18.21
September 22 1999	287.25	6.4	-0.203	-5.2148	-4.2621	23.26	18.13
September 24 1999	287.25	6.4	-1.437	-4.4113	-4.2361	23.36	18.22
September 27 1999	287.35	6.37	-2.976	-3.9306	-4.2303	22.76	17.65
October 8 1999	286.05	6.68	-4.6	-3.6381	-4.063	23.99	18.41
October 11 1999	286.05	6.96	-4.498	-3.6099	-4.0562	25.6	19.68
October 15 1999	285.95	7.32	-4.7	-3.6958	-4.0325	27.37	21
October 22 1999	285.35	7.35	-4.269	-3.6936	-4.021	27.81	21.4
October 29 1999	285.35	7.36	-3.864	-3.5836	-4.0095	28.23	21.8
November 4 1999	285.35	7.4	-3.915	-3.5536	-4.0016	28.46	21.98
November 10 1999	284.55	7.6	-3.921	-3.5867	-3.9871	29.52	22.79
November 15 1999	283.85	7.68	-4.098	-3.6275	-3.9739	29.82	22.99
November 21 1999	282.85	7.74	-4.17	-3.6114	-3.9589	30.14	23.23
November 30 1999	282.65	7.85	-4.133	-3.6294	-3.9305	30.78	23.72
December 6 1999	282.65	7.87	-4.083	-3.589	-3.9465	30.93	23.86
December 15 1999	282.15	7.9	-4.093	-3.5524	-3.9384	31.14	24.02
December 23 1999	281.25	7.94	-4.047	-3.643	-3.9465	31.28	24.12
January 7 2000	281.35	8.07	-3.999	-3.7465	-3.9647	31.88	24.58
January 19 2000	279.75	8.01	-3.893	-3.8189	-4.0815	31.39	24.22
February 2 2000	279.45	8.17	-4.042	-3.8464	-4.0153	32.22	24.83
February 9 2000	280.15	8.14	-4.017	-3.827	-4.0813	32	24.69
February 15 2000	280.35	8.16	-4.036	-3.884	-4.1167	32	24.67
March 31 2000	281.65	8.02	-4.154	-3.7619	-4.0837	31.34	24.16
April 4 2000	281.55	7.9	-4.069	-3.6635	-4.0947	30.82	23.8

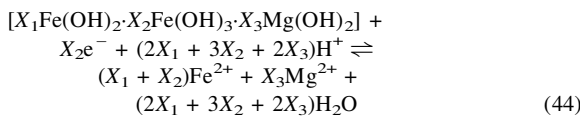
Table 5. (contd.)

Date	T (K)	pH	pe	$\log(\text{Fe}^{2+})$	$\log(\text{Mg}^{2+})$	$\log \text{IAP}_{\text{F1}}$	$\log \text{IAP}_{\text{F2}}$
April 6 2000	281.45	7.87	-3.915	-3.7811	-4.0651	30.68	23.67
April 14 2000	281.45	7.91	-3.898	-3.7022	-4.1409	30.88	23.87
April 20 2000	281.75	7.95	-3.868	-3.8145	-4.1375	31	23.94
May 9 2000	284.95	8.03	-4.264	-3.7276	-4.084	31.36	24.17
May 22 2000	286.05	7.92	-4.144	-3.7362	-4.1214	30.78	23.74
June 5 2000	286.45	7.9	-4.199	-3.8221	-4.1383	30.52	23.53
Average	283.92	7.29	-3.388	-3.6446	-3.9923	28.14	21.78
σ	2.57	0.51	0.856	0.3321	0.1288	2.62	1.99

fougerite1: $\log \text{IAP}_{\text{F1}} = \log(\text{Fe}^{2+}) + \frac{1}{2}\log(\text{Mg}^{2+}) + \frac{2}{3}\log a_w + \frac{3}{2}\text{pe} + \frac{2}{3}\text{pH}$; $\log K_{\text{F1}} = 10.4$, see text

Fougerite2: $\log \text{IAP}_{\text{F2}} = \log(\text{Fe}^{2+}) + \frac{1}{2}\log(\text{Mg}^{2+}) + \frac{2}{3}\log a_w + \frac{3}{2}\text{pe} + \frac{2}{3}\text{pH}$; $\log K_{\text{F2}} = 13.1$, see text

The range of variation of mole fractions is narrow: $\Delta X_1 = \frac{1}{18}$, $\Delta X_2 = \frac{1}{12}$, $\Delta X_3 = \frac{5}{36}$. In the narrow range where green rusts are stable $X_2 = \frac{1}{44}$, and according to our assumption, μ is minimal and can be considered as constant, so that as a first approximation, fougerite can be approximated as a solid of fixed composition ($\mu \equiv \mu^o$) and the equilibrium reaction simply written in the classical way, for which it is convenient to use mole fractions:



and to which mass-action law can be directly applied as:

$$(X_1 + X_2)\log(\text{Fe}^{2+}) + X_3\log(\text{Mg}^{2+}) + X_2\text{pe} + (2X_1 + 3X_2 + 2X_3)\text{pH} = \log K \quad (45)$$

where $\log K$ is given by:

$$\log K = -\frac{1}{(\ln 10)RT}[(X_1 + X_2)\Delta_f G^o(\text{Fe}_{\text{aq.}}^{2+}) + X_3\Delta_f G^o(\text{Mg}_{\text{aq.}}^{2+}) + (2X_1 + 3X_2 + 2X_3)\Delta_f G^o(\text{H}_2\text{O}_l) - \mu] \quad (46)$$

in which μ is the chemical potential of the solid, and can be computed from our model, using equation 31, the values of the parameters reported in Table 4 and the values of X_i determined above. The computations are made at 298.15 K and consistent with $\mu^o(\text{Fe}^{2+}, \text{aq.}) = -91.5 \text{ kJ mol}^{-1}$ from Bourrié *et al.* (1999), $\mu^o(\text{Mg}^{2+}, \text{aq.}) = -455.41 \text{ kJ mol}^{-1}$ from Bratsch (1989).

The results obtained are $\mu(\text{F1}) = -812.7 \text{ kJ mol}^{-1}$ and $\mu(\text{F2}) = -765.2 \text{ kJ mol}^{-1}$, from which one obtains, for 'fougerite1':

$$\log(\text{Fe}^{2+}) + \frac{1}{2}\log(\text{Mg}^{2+}) + \frac{2}{3}\log a_w + \frac{3}{2}\text{pe} + \frac{2}{3}\text{pH} = \log K_{\text{F1}} = 10.4 \quad (47)$$

and for 'fougerite2':

$$\log(\text{Fe}^{2+}) + \frac{1}{2}\log(\text{Mg}^{2+}) + \frac{2}{3}\log a_w + \frac{3}{2}\text{pe} + \frac{2}{3}\text{pH} = \log K_{\text{F2}} = 13.1 \quad (48)$$

Activities were computed, providing for formation of ion pairs and for correction of deviation of non-ideality

of electrolyte solutions at the actual temperature of the samples, by using the EQUIL(T) code, as earlier (Bourrié *et al.*, 1999) for a set of 68 soil solutions sampled in Fougères from February 1999 to June 2000 (Feder, 2001). The complete set of data is given in Table 5.

Solutions are largely undersaturated with respect to all three pure end-members. For the two types of fougerite considered: $\log \text{IAP}_{\text{F1}}$ values range from 22.8 to 32.2 (av. = 28.14, $\sigma = 2.62$); $\log \text{IAP}_{\text{F2}}$ values range from 17.6 to 24.8 (av. = 21.78, $\sigma = 2$).

The uncertainty in the values of $\log K$ obtained for the mineral must be about $\pm 4 \text{ kJ mol}^{-1}$, for 1 Fe atom in the mineral, which gives ± 0.7 logarithmic units. Large supersaturations are observed for both 'fougerite1' and 'fougerite2'. The larger the Mg content in the mineral, the larger the supersaturations observed. It can thus be concluded that fougerite forms from solutions largely oversaturated, when Fe^{3+} coprecipitates with Fe^{2+} and Mg^{2+} . The presence of Mg has a very strong stabilizing effect on the mineral.

IMPLICATIONS CONCERNING THE GENESIS OF FOUGERITE, Mg AND Fe GEOCHEMISTRY

The implications for Fe and Mg geochemistry are as follows: due to its extremely small solubility, Fe(III) is absent from aqueous solution; when Fe oxides are reduced, Fe^{2+} is released in solution, in milieus where Mg^{2+} is generally present too. When oxidation occurs, Fe^{3+} precipitates with Fe^{2+} and Mg^{2+} to give rise to fougerite. The initial Fe/Mg in the mineral is fixed by the composition of the solution. Then, fougerite is oxidized progressively at constant Mg mole ratio, (path from N to P, Figure 3). When the Fe(III) mole ratio reaches its maximum $X_2 = \frac{1}{3}$, fougerite dissolves or recrystallizes and lepidocrocite or goethite forms. The new consequence is that Mg geochemistry is involved: synthetic GR have been considered mainly with respect to their capacity to absorb anions in a first step and then to release them back to solutions. The same occurs here with Mg.

ACKNOWLEDGMENTS

We acknowledge the support of INRA, of the French "Programme National de Recherche Sol et Erosion" (PNSE), of the French Ministry of Education for the grant to F. Feder, and of the European Union (European Fund for Regional Development), and the help of Dr G. Klingelhöfer and Dr B. Bernhardt for the acquisition of Mössbauer *in situ* spectra. Comments by Dr S. Aja, an anonymous referee and Dr J. Amonette are gratefully acknowledged.

REFERENCES

- Abdelmoula, M., Trolard, F., Bourrié, G. and Génin, J.-M.R. (1998) Evidence for the Fe(II)-Fe(III) green rust Fouggerite mineral occurrence in a hydromorphic soil and its transformation with depth. *Hyperfine Interactions*, **112**, 235–238.
- Altmeier, M., Metz, V., Neck, V., Müller, R. and Fanghänel, Th. (2003) Solid-liquid equilibria of $Mg(OH)_2^{(cr)}$ and $Mg(OH)_3Cl \cdot 4H_2O^{(cr)}$ in the system Mg-Na-H-OH-Cl-H₂O at 25°C. *Geochimica et Cosmochimica Acta*, **67**, 3595–3601.
- Arden, T.V. (1950) The solubility products of ferrous and ferrosic hydroxides. *Journal of the Chemical Society*, 882–885.
- Bernal, J.D., Dasgupta, D.R. and Mackay, A.L. (1959) The oxides and hydroxides of iron and their structural inter-relationships. *Clay Minerals Bulletin*, **24**, 882–885.
- Bourrié, G. (1983) Rôle des composés amorphes dans le contrôle de la composition chimique des solutions du sol. *Science du Sol*, **3-4**, 195–204.
- Bourrié, G., Trolard, F., Génin, J.-M.R., Jaffrezic, A., Maître, V. and Abdelmoula, M. (1999) Iron control by equilibria between hydroxy-Green Rusts and solutions in hydromorphic soils. *Geochimica et Cosmochimica Acta*, **63**, 3417–3427.
- Bratsch, S.G. (1989) Standard electrode potentials and temperature coefficients in water at 298.15 K. *Journal of Physical and Chemical Reference Data*, **18**, 1–21.
- Davies, P.K. and Navrotsky, A. (1983) Quantitative correlations of deviations from ideality in binary and pseudobinary solid solutions. *Journal of Solid State Chemistry*, **46**, 1–22.
- Détournay, J., De Miranda, L., Dérié, R. and Ghodsi, M. (1975) The region of stability of green rust II in the electrochemical E-pH equilibrium diagram of iron in sulphate medium. *Corrosion Science*, **15**, 295–306.
- Drissi, S.H., Refait, Ph. and Génin, J.-M.R. (1994) The oxidation of $Fe(OH)_2$ in the presence of carbonate ions: structure of carbonate green rust one. *Hyperfine Interactions*, **90**, 395–400.
- Drissi, S.H., Refait, Ph., Abdelmoula, M. and Génin, J.-M.R. (1995) Preparation and thermodynamic properties of Fe(II)-Fe(III) hydroxide-carbonate (green rust one). Pourbaix diagram of iron in carbonate-containing aqueous media. *Corrosion Science*, **37**, 2025–2041.
- Feder, F. (2001) Dynamique des processus d'oxydo-réduction dans les sols hydromorphes – monitoring *in situ* de la solution du sol et des phases solides ferrifères. Thèse, Université d'Aix-Marseille III, Aix-en-Provence, France, 200 pp.
- Génin, J.-M.R., Olowe, A.A., Refait, Ph. and Simon, L. (1996a) On the stoichiometry and Pourbaix diagram of Fe(II)-Fe(III) hydroxy-sulphate or sulphate containing green rust 2; an electrochemical and Mössbauer spectroscopy study. *Corrosion Science*, **38**, 1751–1762.
- Génin, J.-M.R., Simon, L. and Refait, Ph. (1996b) Existence of sulphite-containing green rust one. Pp. 51–54 in: *Proceedings ICAME 95* (I. Ortalli, editor). SIF, Bologna, Italy.
- Génin, J.-M.R., Abdelmoula, M., Refait, Ph. and Simon, L. (1998a) Comparison of the Green Rust Two lamellar double hydroxide class with the Green Rust One pyroaurite class: Fe(II)-Fe(III) sulphate and selenate hydroxides. *Hyperfine Interactions*, **C**, **3**, 313–316.
- Génin, J.-M.R., Bourrié, G., Trolard, F., Abdelmoula, M., Jaffrezic, A., Refait, Ph., Maître, V., Humbert, B. and Herbillon, A. (1998b) Thermodynamic equilibria in aqueous suspensions of synthetic and natural Fe(II)-Fe(III) Green Rusts: occurrences of the mineral in hydromorphic soils. *Environmental Science and Technology*, **32**, 1058–1068.
- Génin, J.-M.R., Refait, Ph., Bourrié, G., Abdelmoula, M. and Trolard, F. 2001 Structure and stability of the Fe(II)-Fe(III) green rust "fouggerite" mineral and its potential for reducing pollutants in soil solutions. *Applied Geochemistry*, **16**, 559–570.
- Girard, A. and Chaudron, G. (1935) Sur la constitution de la rouille. *Comptes-Rendus de l'Académie des Sciences, Paris*, **200**, 127–129.
- Hansen, H.C.B. (1989) Composition, stabilisation and light absorption of Fe(II)-Fe(III) hydroxycarbonate (green rust). *Clay Minerals*, **24**, 663–669.
- Hansen, H.C.B. and Taylor, R.M. (1991) Formation of synthetic analogues of double metal-hydroxy carbonate minerals under controlled pH conditions: II. The synthesis of desautelsite. *Clay Minerals*, **26**, 507–525.
- Hashimoto, K. and Misawa, T. (1973) The solubility of $\gamma FeOOH$ in perchloric acid at 15 °C. *Corrosion Science*, **13**, 229–231.
- Jolivet, J.P. (1994) *De la solution à l'oxyde — Condensation des cations en solution aqueuse — Chimie de surface des oxydes*. InterEditions / CNRS Editions, Paris, 387 pp.
- Koritnig, S. and Susse, P. (1975) Meixnerit, $Mg_6Al_2(OH)_{18} \cdot 4H_2O$, ein neues Magnesium-Aluminium-Hydroxid-Mineral. *Tschermaks Mineralogische Petrologische Mitteilungen*, **22**, 79–87.
- Mascolo, G. and Marino, O. (1980) A new synthesis and characterization of magnesium-aluminium hydroxides. *Mineralogical Magazine*, **43**, 619–621.
- Murad, E. and Taylor, R.M. (1984) The Mössbauer spectra of hydroxycarbonate green rusts. *Clay Minerals*, **19**, 77–83.
- Olowe, A.A. and Génin, J.-M.R. (1991) The mechanism of oxidation of Fe(II) hydroxide in sulphated aqueous media: importance of the initial ratio of the reactants. *Corrosion Science*, **32**, 965–984.
- Ponnampерuma, F.N., Tianco, E.M. and Loy, T. (1967) Redox equilibria in flooded soils: I. The iron hydroxide system. *Soil Science*, **103**, 374–382.
- Prigogine, I. and Defay, R. (1946) *Thermodynamique chimique conformément aux méthodes de Gibbs et De Donder*. Dunod, Paris, tome I, 348 pp., tome II, 430 pp.
- Refait, Ph., Abdelmoula, M. and Génin, J.-M.R. (1998a) Mechanisms of formation and structure of green rust one in aqueous corrosion of iron in the presence of chloride ions. *Corrosion Science*, **40**, 1547–1560.
- Refait, Ph., Abdelmoula, M., Trolard, F., Génin, J.-M.R., Ehrhardt, J.-J. and Bourrié, G. (2001) Mössbauer and XAS study of a green rust mineral; the partial substitution of Fe^{2+} by Mg^{2+} . *American Mineralogist*, **86**, 731–739.
- Refait, Ph., Bon, C., Simon, L., Bourrié, G., Trolard, F., Bessière, J. and Génin, J.-M.R. (1999) Chemical composition and Gibbs standard free energy of formation of Fe(II)-Fe(III) hydroxysulphate green rust and Fe(II) hydroxide. *Clay Minerals*, **34**, 499–510.
- Refait, Ph., Charton, A. and Génin, J.-M.R. (1998b) Identification, composition, thermodynamic and structural properties of a pyroaurite-like iron(II)-iron(III) hydroxy-oxalate Green Rust. *European Journal of Solid State Inorganic Chemistry*, **35**, 655–666.

- Refait, Ph. and Génin, J.-M.R. (1993) The oxidation of Ni(II)-Fe(II) hydroxides in chloride-containing aqueous media. *Corrosion Science*, **34**, 2059–2070.
- Refait, Ph., Simon, L., Louis, C. and Génin, J.-M.R. (2000) Reduction of SeO_4^{2-} anions and anoxic formation of iron(II)-iron(III) hydroxy-selenite green rust. *Environmental Science and Technology*, **34**, 819–825.
- Roussel, H., Briois, V., Elkaim, E., de Roy, A. and Besse, J.P. (2000) Cationic order and structure of [Zn-Cr-Cl] and [Cu-Cr-Cl] layered double hydroxides: a XRD and EXAFS study. *Journal of Physical Chemistry*, **B25**, 5915–5953.
- Shannon, R.D. (1976) Revised effective ionic radii and systematic studies of interatomic distances in halides and chalcogenides. *Acta Crystallographica*, **A32**, 751–767.
- Simon, L., François, M., Refait, Ph., Renaudin, G., Lelaurain, M. and Génin, J.-M.R. (2003) Structure of the Fe(II-III) layered double hydroxysulphate green rust two from Rietveld analysis. *Solid State Sciences*, **5**, 327–334.
- Simon, L., Refait, Ph. and Génin, J.-M.R. (1998) Transformation of Fe(II)-Fe(III) hydroxysulphite into hydroxysulphate Green Rusts. *Hyperfine Interactions*, **112**, 217–220.
- Stampfl, P.P. (1969) Ein basisches Eisen-II-III-Karbonat in Rost. *Corrosion Science*, **9**, 185–187.
- Taylor, R.M. (1981) Color in soils and sediments. A review. In: "International Clay Conference 1981" (H. Van Olphen ed.), *Developments in Sedimentology*, **35**, p. 749–761, Elsevier, Amsterdam.
- Taylor, R.M. and MacKenzie, R.M. (1980) The influence of aluminum on iron oxides. VI. The formation of Fe(II)-Al(III) hydroxy-chlorides, -sulfates, and -carbonates as new members of the pyroaurite group and their significance in soils. *Clays and Clay Minerals*, **28**, 179–187.
- Trolard, F., Abdelmoula, M., Bourrié, G., Humbert, B. and Génin, J.-M.R. (1996) Mise en évidence d'un constituant de type "rouilles vertes" dans les sols hydromorphes - Proposition de l'existence d'un nouveau minéral : la "fougérite". *Comptes-Rendus de l'Académie des Sciences, Paris*, **323, IIa**, 1015–1022.
- Trolard, F., Génin, J.-M.R., Abdelmoula, M., Bourrié, G., Humbert, B. and Herbillon, A. (1997) Identification of a green rust mineral in a reductomorphic soil by Mössbauer and Raman spectroscopies. *Geochimica et Cosmochimica Acta*, **61**, 1107–1111.
- Vucelic, M., Jones, W. and Moggridge, G.D. (1997) Cation ordering in synthetic layered double hydroxides. *Clays and Clay Minerals*, **45**, 803–813.
- Vysotskii, G.N. (1905) Gley. *Pochvovedeniye*, **4**, 291–327. (original paper in Russian). (1999) Gley. An abridged version of Vysotskii (1905) on the 257th Anniversary of the Russian Academy of Sciences. *Eurasian Soil Science*, **32**, 1063–1068.
- Wagman, D.D., Evans, W.H., Parker, V.B., Schumm, R.H., Halow, L., Bailey, S.M., Churney, K.L. and Nuttall, R.L. (1982) The NBS Tables of chemical thermodynamic properties. Selected values for inorganic and C1 and C2 organic substances in SI units. *Journal of Physical and Chemical Reference Data, Supplement n°2*, 11.

(Received 23 January 2003; revised 6 January 2004;
Ms. 753; A.E. James E. Amonette)